V_H and C_H are used to refer to the corresponding regions of heavy chains [see *Bull. Wld. Hlth. Org.* **41**, 975 (1969)].
2. H. Köhler, A. Shimizu, C. Paul, F. W. Putnam, *Science* **169**, 56 (1970).
3. M. Wikler, H. Köhler, T. Shinoda, F. W. Putnam, *ibid.* **163**, 75 (1969).
4. C. Paul, A. Shimizu, H. Köhler, F. W. Putnam, *ibid.* **172**, 69 (1971).
5. E. M. Press and N. M. Hogg, *Biochem. J.* **117**, 641 (1970).
6. B. A. Cunningham, M. N. Pflumm, U. Rutishauser, G. M. Edelman, *Proc. Nat. Acad. Sci. U.S.* **64**, 997 (1969).
7. L. Hood and D. W. Talmage, *Science* **168**, 325 (1970).
8. H. Köhler, A. Shimizu, C. Paul, V. Moore, F. W. Putnam, *Nature* **227**, 1318 (1970). In this paper the symbols V_{HI}, V_{HII}, V_{HIII}, and V_{HIV} were proposed for the four major subgroups of variable sequence in heavy chains and examples of the subgroup sequences were given.
9. The first peak contained fragments bound together by disulfide bridges; the second comprised fragments F1, F2, and F3, which together constitute the first 105 residues in the sequence (*3*) (Fig. 1). The tyrosine-rich peptide F4 was isolated in good yield from the latter part of the Sephadex eluate. The material in the first peak was reduced with 0.2*M* mercaptoethanol in 6*M* guanidine and aminoethylated with ethylenimine to break the disulfide bonds and was reapplied to Sephadex G-100. This separated the κ light chain, fragment F5, and the NH_2-terminal portion of F6. In addition, the whole μ chain was cleaved with trypsin and with thermolysin in separate experiments (*2*). The whole μ chain and the Fcμ fragment were also cleaved with CNBr, reduced in 6*M* guanidine, and alkylated with ethylenimine, and the resultant CNBr fragments were separated on Sephadex. Gel filtration, ion-exchange chromatography, paper electrophoresis, and paper chromatography were used to purify chymotryptic peptides obtained from F5, F6, and Fcμ, tryptic peptides from the whole μ chain and from the CNBr fragments of the whole μ chain and of Fcμ, and thermolysin peptides from the whole μ chain. These were in addition to the tryptic and chymotryptic peptides from F1, F2, and F3 that were earlier sequenced (*3*) and the tryptic and thermolysin peptides that led to the sequence of the κ light chain (*2*). The Beckman sequencer model 890 was used to determine the NH_2-terminal sequence for 10 to 47 steps of various unblocked fragments. The sequence of the tryptic, chymotryptic, and thermolysin peptides was determined by methods already described by us [K. Titani, M. Wikler, F. W. Putnam, *J. Biol. Chem.* **245**, 2142 (1970); T. Shinoda, K. Titani, F. W. Putnam, *ibid.*, p. 4463].
10. Abbreviations for amino acid residues: Lys, lysine; His, histidine; Arg, arginine; Asp, aspartic acid; Asn, asparagine; Asx, aspartic acid or asparagine, identity not established; Thr, threonine; Ser, serine; Glu, glutamic acid; Gln, glutamine; Glx, glutamic acid or glutamine, identity not established; Pro, proline; Gly, glycine; Ala, alanine; Val, valine; Ile, isoleucine; Leu, leucine; Tyr, tyrosine; Phe, phenylalanine; Trp, tryptophan; Cys, half-cystine. The first amino acid of the chain is designated Asp-1 and so forth.
11. A. Shimizu, F. W. Putnam, C. Paul, J. R. Clamp, I. Johnson, *Nature New Biol.* **231**, 73 (1971).
12. G. M. Edelman, B. A. Cunningham, W. E. Gall, P. D. Gottlieb, U. Rutishauser, M. J. Waxdal, *Proc. Nat. Acad. Sci. U.S.* **63**, 78 (1969).
13. H. Ponstingl, J. Schwarz, W. Reichel, N. Hilschmann, *Z. Physiol. Chem.* **351**, 1591 (1970).
14. For a matrix table of the identities and a "phylogenetic tree" of the variable sequence regions of human heavy chains, see F. W. Putnam, A. Shimizu, C. Paul, T. Shinoda, H. Köhler, *Ann. N.Y. Acad. Sci.*, in press.
15. A. C. Wang, J. R. L. Pink, H. H. Fudenberg, J. Ohms, *Proc. Nat. Acad. Sci. U.S.* **66**, 657 (1970).
16. R. G. Fruchter, S. A. Jackson, L. E. Mole, R. R. Porter, *Biochem. J.* **116**, 249 (1970).
17. A. Bourgois and M. Fougereau, *Fed. Eur. Biochem. Soc. FEBS Lett.* **8**, 265 (1970).
18. N. O. Thorpe and S. J. Singer, *Biochemistry* **8**, 4431 (1969); R. R. Porter, in *Homologies in Enzymes and Metabolic Pathways and Metabolic Alterations in Cancer*, W. J. Whelan and J. Schultz, Eds. (North-Holland, Amsterdam, 1970).
19. O. Smithies, D. N. Gibson, E. M. Fanning, M. E. Percy, D. M. Parr, G. E. Connell, *Science* **172**, 574 (1971).
20. D. Beale and N. Buttress, *Biochim. Biophys. Acta* **181**, 250 (1969); D. Beale and A. Feinstein, *Biochem. J.* **112**, 187 (1969); H. Metzger, *Adv. Immunol.* **12**, 57 (1970).
21. S. Brenner and C. Milstein, *Nature* **211**, 242 (1966).
22. B. Frangione, C. Milstein, E. C. Franklin, *Biochem. J.* **106**, 15 (1968).
23. M. B. Perry and C. Milstein, *Nature* **228**, 934 (1970).
24. K. J. Turner and J. J. Cebra, *Biochemistry* **10**, 9 (1971); B. K. Birshtein, Q. Z. Hussain, J. J. Cebra, *ibid.*, p. 18.
25. C. De Preval, J. R. L. Pink, C. Milstein, *Nature* **228**, 930 (1970).
26. We had earlier suggested (*3*) that the 17-residue fragment F9 was homologous to a segment corresponding to residues 338 through 355 in rabbit and human γ chains. However, with this alignment the homology between the μ and γ chains diminishes rapidly after the 17-residue segment. On the other hand, the homology is about 35 percent for a segment of 70 residues if the half-cystines in the last intrachain bridge of the μ and γ1 chains are aligned, that is, Cys-425 in the Eu γ1 chain and the next to the last half-cystine in the μ chain. Yet, in this alignment an additional 19 amino acid residues in the μ chain extend beyond the C-terminal glycine of the γ1 chain. A similar result is obtained when the μ chain is compared with other subclasses of human γ chains and with animal γ chains. This extension has one carbohydrate prosthetic group and one interchain disulfide bridge that are unique to the μ chain.
27. F. W. Putnam, K. Titani, M. Wikler, T. Shinoda, *Cold Spring Harbor Symp. Quant. Biol.* **32**, 9 (1967); R. L. Hill, R. Delaney, R. E. Fellows, Jr., H. E. Lebovitz, *Proc. Nat. Acad. Sci. U.S.* **56**, 1762 (1966).
28. M. O. Dayhoff, *Atlas of Protein Structure and Sequence 1969* (National Biomedical Research Foundation, Silver Spring, Md., 1969).
29. A joining piece (J piece) first detected in human IgA immunoglobulin (*30*) is also present in low amount in human IgM (*31*). Dr. M. Koshland and M. Halpern of the University of California, Berkeley, have analyzed samples of our proteins and they have informed us that the J piece is present in a ratio of about one per pentamer in whole IgM Ou and in its Fcμ fragment but is absent in the Fabμ fragment. The J piece is not identified in Fig. 1 but is presumably attached through the intersubunit disulfide bridge not shown in the figure.
30. M. S. Halpern and M. E. Koshland, *Nature* **228**, 1276 (1970).
31. J. Mestecky, J. Zikan, W. T. Butler, *Science* **171**, 1163 (1971).
32. M. Wikler, K. Titani, T. Shinoda, F. W. Putnam, *J. Biol. Chem.* **242**, 1668 (1967); F. W. Putnam, T. Shinoda, K. Titani, M. Wikler, *Science* **157**, 1050 (1967).
33. We thank J. Madison, M. Kawahara, P. Keim, and G. McCloskey for technical assistance and Dr. John L. Fahey, NIH Clinical Center, Bethesda, Md., for plasma from patient Ou. Supported by grant CA-08497 from NIH and GB 18483 from NSF.
* Present address: Department of Pathology, University of Chicago, Chicago, Ill. 60637.

1 April 1971; revised 24 May 1971 ■

Core Binding Energy Difference between Bridging and Nonbridging Oxygen Atoms in a Silicate Chain

Abstract. *The x-ray photoelectron spectra of the oxygen 1s level of olivines contain a single component whereas those of pyroxenes contain two components with an intensity ratio of 2 : 1 and an energy separation of about 1 electron volt. We interpret these two components to be the result of the binding energy differences between nonbridging and bridging oxygen atoms within a silicate chain in the pyroxene structure.*

There have been many photoelectron spectroscopic studies of the shift in the binding energy of core electrons due to various chemical effects such as valence states, bond character, and spin-exchange splitting (*1*). In the second (*2*) of a series of three articles entitled "Molecular Spectroscopy by Means of ESCA" (Electron Spectroscopy for Chemical Analysis) (*2, 3*) Lindberg and his co-workers presented specific correlations between the binding energy of the core electrons of sulfur and the structure of sulfur compounds. We have now observed shifts in the binding energy of the 1*s* level of oxygen atoms caused by the differences in the local environment of oxygen atoms within a silicate chain in the pyroxene structure.

The photoelectron spectra were obtained in a newly designed electrostatic analyzer situated in an oil-free vacuum system with operating pressure in the 1×10^{-8} torr region. Although the spectrometer system is capable of producing 1.35 ev half-width for the photoelectron peak from the $4f_{7/2}$ level of gold with Al$K\alpha_{1,2}$ excitation, its resolution was degraded to 2.2 ev for the experiment reported here in order to enhance the signal-to-noise ratio. The samples were in the form of fine powders (< 400 mesh). An extremely thin layer of the powdered sample was brushed onto an aluminum foil substrate, one side of which was covered with several monolayers of adhesive. Because of the presence of surface contaminants each sample was sputter-cleaned with Ar^+-bombardment at 1.5 kev and 20 μm pressure in an antechamber immediately before measurements. The time interval between the end of Ar^+-bombardment and the beginning of measurements in the high 10^{-8} torr range was approximately 6 minutes.

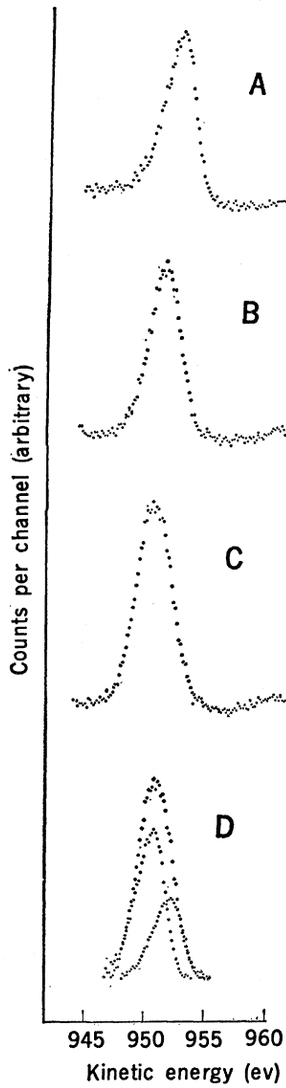

Fig. 1. Oxygen 1*s* photoelectron spectra: (A) Fe_2O_3; (B) Fe-Mg-olivine; (C) orthopyroxene; (D) computer-resolved orthopyroxene.

In the study reported here sets of three samples were mounted on a rotatable sample holder to ensure an identical experimental environment for each set. The effect of charging on insulating samples was investigated at length but none was observed with our method of sample preparation.

The oxygen 1*s* photoelectron spectra of Fe_2O_3, Fe-Mg-olivine, $[(Fe_{0.40}Mg_{0.60})_2SiO_4]$, and orthopyroxene $[(Fe_{0.80}Mg_{0.20})_2Si_2O_6]$ are shown in Fig. 1. The Fe_2O_3 spectrum serves as a standard for line shape and also as a position reference. A similar set of spectra was also collected for Fe_2O_3, Ca-Fe-olivine ($CaFeSiO_4$), and Ca-pyroxene $[(Ca_{0.20}Fe_{0.40}Mg_{0.40})_2Si_2O_6]$. We note the following features in the spectra of Fig. 1:

1) The width of the oxygen 1*s* line from Fe_2O_3 (Fig. 1A) is identical to that of the Fe-Mg-olivine (Fig. 1B); and both are narrower than that of orthopyroxene (Fig. 1C).

2) The binding energy of the oxygen 1*s* electrons is lowest for Fe_2O_3 and highest for orthopyroxene, with the value for Fe-Mg-olivine intermediate between those for Fe_2O_3 and orthopyroxene (see also Fig. 2).

3) The orthopyroxene oxygen curve (Fig. 1C) can be resolved into two components with an intensity ratio of about 2 : 1 and a separation of (1.35 ± 0.15) ev (Fig. 1D) when either Fig. 1A or Fig. 1B is used as a standard. The deconvolution was performed by means of a generalized curve-fitting computer program (*4*) compiled for this purpose.

We also observed these same general features in the other set of samples consisting of Fe_2O_3, Ca-Fe-olivine, and Ca-pyroxene.

In Fig. 2 we indicate the relative shifts in binding energy of the oxygen 1*s* level in the four silicate samples with reference to that of Fe_2O_3. The uncertainties in the energy values are ± 0.15 ev. Our interpretations of these shifts are as follows:

1) Fe_2O_3 has a close-packed hexagonal structure with only one type of Fe–O bond. Hence one expects a single-component oxygen 1*s* photoelectron line whose shape and width can be used as a standard to resolve multiple-component lines from other samples. Since the relative binding energy shift is of interest here, its position is used as a reference for the other samples.

2) The isolated SiO_4 tetrahedron as it occurs in the structures of Fe-Mg-olivine and Ca-Fe-olivine is shown in Fig. 3A. The Si–O bond length for both olivines has been established by x-ray diffraction studies (*5*). Since there is only one type of Si–O bond in this structure, one again expects a single-component oxygen 1*s* line. This is indeed the case when one compares the shape and width of Fig. 1B (Fe-Mg-olivine) with those of Fig. 1A (Fe_2O_3). The oxygen 1*s* binding energies in the olivines are higher than that in Fe_2O_3, an indication of a more covalent bonding character for the Si–O bond in olivine.

3) The single silicate (Si_2O_6) chain as it occurs in the structures of orthopyroxene and Ca-pyroxene is shown in Fig. 3B. There are two types of Si–O bonds in this case, namely, those in-

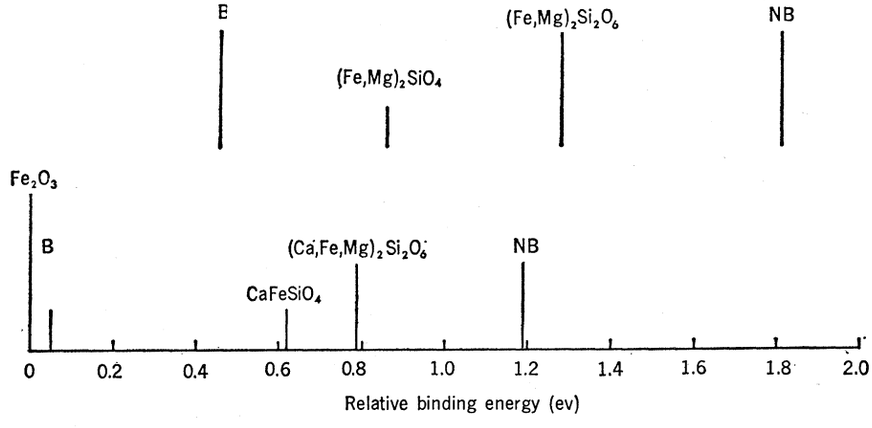

Fig. 2. Relative binding energy shifts of the oxygen 1*s* level in olivines and pyroxenes with reference to Fe_2O_3. Positions indicate the center of the background-subtracted peaks; *NB* and *B* indicate, respectively, the computer-resolved peak positions of the nonbridging oxygen atoms. The higher binding energy in Fig. 2 corresponds to the lower kinetic energy in Fig. 1.

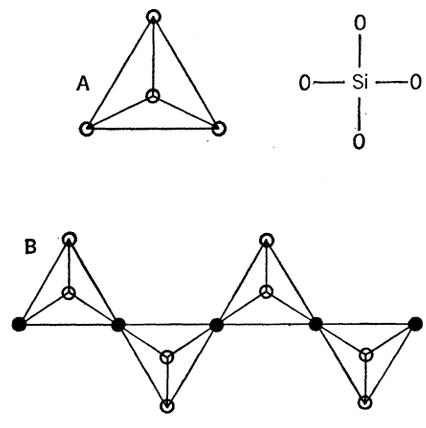

Fig. 3. Isolated silicate structures in olivines and pyroxenes: (A) SiO_4 tetrahedron in olivines; (B) Si_2O_6 chain in pyroxenes; (solid circles) bridging oxygen atoms; (open circles) nonbridging oxygen atoms.

volving the bridging and the nonbridging oxygens. The average bond lengths, as established by x-ray diffraction studies, are, for the bridging oxygens, 1.67 and 1.65 Å for chains A and B in orthopyroxene (*6*), and 1.68 Å in Ca-pyroxene (*7*). For the nonbridging oxygens the average bond lengths are 1.60 Å for both chains A and B in orthopyroxene (*6*), and 1.59 Å in pyroxene ($CaMgSi_2O_6$) (*7*). Thus the Si–O bond lengths for the bridging oxygens are roughly 0.07 Å longer than those for the nonbridging oxygens. The population ratio of the nonbridging to bridging oxygens is 2 : 1. As can be seen from Fig. 1D, the oxygen 1*s* spectrum of orthopyroxene does indeed consist of two components with an intensity ratio of about 2 : 1. The same intensity ratio was also observed in the deconvoluted oxygen spectrum from Ca-pyroxene. Furthermore, since longer bond lengths indicate in general a more ionic bonding character, one expects the bridging oxygens to have lower binding energy than the nonbridging oxygens. This result is also clearly demonstrated in Figs. 1D and 2.

4) The 1*s* level of the oxygen atoms in Ca-pyroxene and Ca-olivine have lower binding energies than those in the Fe-Mg set. This effect is most likely due to the influence of the cations in the crystal structure.

The results presented here show that photoelectron spectroscopy is a useful technique for the systematic study of the correlation between bond lengths and core binding energies among given pairs of atoms, such as Si–O in the silicate chains.

LO I YIN
SUBRATA GHOSE
ISIDORE ADLER

National Aeronautics and Space Administration, Goddard Space Flight Center, Greenbelt, Maryland 20771

References

1. K. Siegbahn *et al., ESCA Atomic, Molecular, and Solid State Structure Studied by Means of Electron Spectroscopy* (Almqvist & Wiksell, Stockholm, 1967); C. S. Fadley, D. A. Shirley, A. J. Freeman, P. S. Bagus, J. V. Mallow, *Phys. Rev. Lett.* **23**, 1397 (1969).
2. B. J. Lindberg, K. Hamrin, G. Johansson, U. Gelius, A. Fahlman, C. Nordling, K. Siegbahn, *Phys. Scripta* **1**, 286 (1970).
3. R. Nordberg, R. G. Albridge, T. Bergmark, U. Ericson, J. Hedman, C. Nordling, K. Siegbahn, B. J. Lindberg, *Ark. Kemi* **28**, 257 (1968); U. Gelius, P. F. Hedén, J. Hedman, B. J. Lindberg, R. Manne, R. Nordberg, C. Nordling, K. Siegbahn, *Phys. Scripta* **2**, 70 (1970).
4. J. I. Trombka, R. Schmadebeck, G. A. Osswald, in preparation.
5. J. D. Birle, G. V. Gibbs, P. B. Moore, J. V. Smith, *Amer. Mineral.* **53**, 807 (1968); H. Onken, *Mineral. Petrogr. Mitt.* **10**, 34 (1965).
6. S. Ghose, *Z. Kristallogr.* **122**, 81 (1965).
7. J. R. Clark, D. E. Appleman, J. J. Papike, *Mineral. Soc. Amer. Spec. Pap. 2* (1969), p. 31.

29 April 1971

Follicle-Stimulating Hormone and the Regulation of Testosterone Secretion in Rabbit Testes

Abstract. *Regulation of testosterone secretion is presumably mediated by interstitial cell–stimulating hormone (ICSH). However, there is little information on the actions of other chemical messengers in regulating testosterone secretion. We have shown that follicle-stimulating hormone augments testosterone secretion stimuated by ICSH in rabbit testes perfused in vitro with an artificial medium.*

Alterations in testosterone secretion are presumably mediated by interstitial cell–stimulating hormone (ICSH), and testosterone is thought to act on the hypothalamo-hypophyseal complex to regulate ICSH release. The fact that testosterone is influenced by a wide variety of signals (*1*) suggests that this mechanism cannot be the sole regulator of testosterone secretion. Similarly, mechanisms discovered in other organ systems imply by extension a multiplicity of controls for regulation of testosterone.

For instance, insulin, hydrocortisone, and prolactin are required to stimulate synthesis of milk protein in mouse mammary glands (*2*); and prolactin, luteinizing hormone, and follicle-stimulating hormone (FSH) are needed to maintain functional corpora lutea in pregnant hamsters (*3*).

Determination of the hormonal factors that regulate testosterone secretion in mammals has been hampered by the lack of a suitable experimental preparation that could be used in examining the effects of chemical messengers on testosterone secretion without interference from extrinsic signals. The continued development of the perfused rabbit testis in vitro (*4, 5*) suggests that this may be the best experimental system in which to examine the effects of a variety of hormones on testosterone secretion. Secretion of testosterone by testes perfused with defibrinated rabbit blood is approximately 500 ng per gram of testis per hour throughout a 6-hour perfusion (*5*). In contrast, secretion by testes perfused with an artificial medium declines during the first 2 hours of perfusion to a basal amount of 50 ng of testosterone per gram of testis per hour (*6*). Addition of ICSH to the artificial medium restores secretion. These observations demonstrate that an artificial medium lacks factors responsible for maintaining testosterone secretion in rabbit testes.

It has been suggested that FSH augments testosterone secretion (*7*), but quantitative measures of such an effect on secretion stimulated by ICSH have not been described. Such studies have

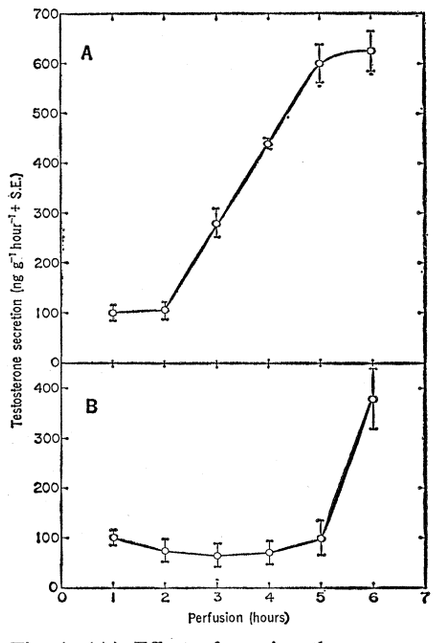

Fig. 1. (A) Effect of varying the concentration of ICSH in artificial medium on hourly rate of testosterone secretion ($n = 4$). The concentrations at successive hours were: 1 hour, 0.0 μg/ml; 2 hours, 0.01 μg/ml; 3 hours, 0.025 μg/ml; 4 hours, 0.05 μg/ml; 5 hours, 0.1 μg/ml; and 6 hours, 1.0 μg/ml. (B) Effect of varying the concentration of FSH in artificial medium on hourly rate of testosterone secretion ($n = 4$). The concentrations at successive hours were: 1 hour, 0.0 μg/ml; 2 hours, 0.01 μg/ml; 3 hours, 0.025 μg/ml; 4 hours, 0.05 μg/ml; 5 hours, 0.1 μg/ml; and 6 hours, 1.0 μg/ml. Gonadotrophins (GTH) were infused directly into the arterial cannula by means of a Sage Micro Pump equipped with a 500-μl Hamilton gas-tight syringe. The concentration of GTH in the syringe was altered at the end of each hour of perfusion. Thus, the same volume of GTH solution was perfused each hour. The volume of fluid added to the arterial cannula never exceeded 120 μl/hour.